Planar force-constant method for lattice dynamics of superstructures

A. Fasolino*
Service National des Champs Intenses du Centre National de la Recherche Scientifique (SNCI-CNRS), Boîte Postale 166X, F-38042 Grenoble CEDEX, France

E. Molinari
Istituto di Acustica "O.M. Corbino," Consiglio Nazionale delle Ricerche, via Cassia 1216, I-00189 Roma, Italy

K. Kunc
Laboratoire de Physique des Solides associé au Centre National de la Recherche Scientifique, Université Pierre et Marie Curie, Tour 13, 4 place Jussieu, F-75230 Paris CEDEX 05, France
(Received 13 September 1989)

We present a simple and accurate method for dealing with phonons in superlattices, and illustrate it with the example of GaAs/AlAs heterostructures. In this approach the vibrations of the superlattice are described in terms of planar force constants, which are determined *ab initio* for one constituent (e.g., GaAs bulk) and extended to the other constituent (e.g., AlAs) by introduction of the "mass and charge approximation." Within this approximation, the dynamical problem of the superlattice is represented as that of an infinite bulk crystal (e.g., GaAs), which is modified by a sequence of *on-site* perturbations. We systematically develop the formalism for the one-dimensional description of phonons propagating along the superlattice growth direction, derive its relation with the general three-dimensional description, and clarify its physical meaning. The representation of the Coulomb interactions in the one-dimensional formalism is described in some detail. Applications of the method to $(GaAs)_m/(AlAs)_n$ superlattices of several thicknesses are discussed.

I. INTRODUCTION

In recent years the interest in the vibrational properties of semiconductor superlattices has been growing very rapidly, most because of the great amount of structural information which can become experimentally accessible by studying phonons via light-scattering experiments. Most of the work has been devoted to $Ga_{1-x}Al_xAs$ systems (see, e.g., the reviews in Ref. 1). In particular, in the last few years the attention has been focused on the role of interfaces: for example, superlattices (SL's) with very sharp[2] or with artificially disordered[3] interfaces have been studied by Raman, in order to clarify the effect of interface inhomogeneities on the spectra; the research on GaAs/AlAs systems has also developed towards ultrathin SL's (Ref. 4) and SL's with more complex periodic or aperiodic stacking sequences.[5] Moreover, the interest is now extending to SL's made of other materials, such as, e.g., Si/Ge (Refs. 6 and 1) or GaAs/InAs,[7] where strain effects are often important.

The first theoretical microscopic understanding of the main features of GaAs/AlAs SL phonon spectra have been provided by modeling the SL structure with a linear chain with first-neighbor interactions.[8–10] Although these models were based on a very simplified description of the bonding in GaAs/AlAs, they were able to describe the main features of phonons propagating along the SL growth direction, namely the appearance of folding in the acoustical frequency range and confinement in the optical range. The success of this simple model results from the fact that the linear-chain equations of motion actually describe the vibrations of a chain of atomic *planes*, which is an exact picture of phonons propagating in the growth direction. Indeed, the transformation of the three-dimensional (3D) dynamical problem into three one-dimensional (1D) (linear-chain) problems is exact, as the high-symmetry atomic planes are made of a single atomic species and vibrate as a whole.

After the more detailed experimental data obtained by Raman were gathered—giving information mainly on modes propagating along the growth direction—we have put forward a model[11–13] which is capable of providing a more quantitative description of both optical and acoustical branches, without abandoning the conceptual simplicity of the linear-chain approach. This can be achieved by use of interplanar force constants based on a more refined description of the bulk components, such as long-range force constants derived by first-principles calculations, as will be shown in detail in the following sections.

Our approach uses as its starting point results obtained in first-principles calculations; however, only a very simple formalism is then employed for the description of the phonons. The size of the problem remains tractable even when dealing with thick SL's,[14,15] and the method has already proven its usefulness in describing other superlattices, such as InAs/GaSb (Refs. 16–18) and Si/Ge.[18–20] The method satisfies two important requirements: (i) it reproduces the bulk-phonon spectra of the SL constituents, and (ii) it describes the two constituent materials in terms of the same interactions: their difference is reduced to different on-site properties, namely masses and effective charges ("mass and charge approximation"). It is then naturally suitable to treat layered materials and

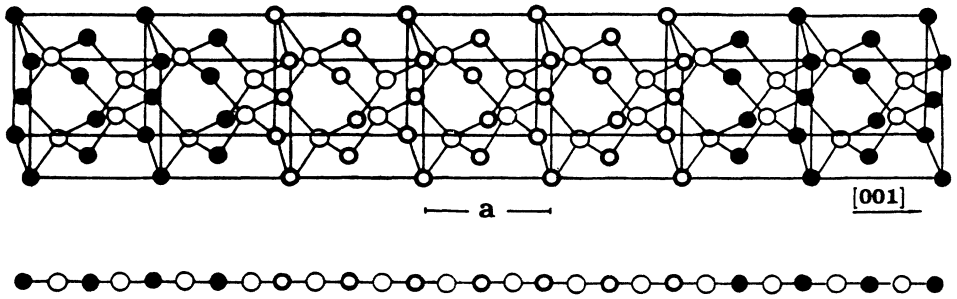

FIG. 1. Structure of the three-dimensional unit cell of a $(GaAs)_7/(AlAs)_7$ (001) superlattice. The projection onto a one-dimensional chain is shown at the bottom. Larger circles represent As atoms (→ atomic planes), smaller solid and open circles represent Ga and Al atoms (→ atomic planes). a is the bulk lattice parameter.

their interfaces.

The purpose of this paper is to give a detailed derivation of our method, and to provide explicitly the ingredients which are needed to apply it to different situations. In Sec. II we present the bulk lattice dynamics and introduce the "mass and charge approximation" for the bulk constituents. In Sec. III the "mass and charge approximation" is extended to construct the dynamical matrix of GaAs/AlAs SL's. Typical calculated phonon spectra are presented in Sec. IV.

It should be noted that recently full 3D calculations based on models of different complexity[21–26] (rigid-ion model, bond-charge model) have appeared, which can also treat the dispersion along other directions and, in principle, can be extended to include in-plane inhomogeneities. Some of them have contributed, in particular, to the understanding of the microscopic origin of the observed anisotropy of optical modes[27] and SL interface modes propagating parallel to the interfaces. Such interface modes, observed for the first time by Sood *et al.*,[28] were previously interpreted only in terms of macroscopic matching of dielectric functions.[28–30] On the other hand, first-principles calculations performed on the thinnest superlattices are starting to appear.[31] Being more complex, these approaches have only been applied to a limited number of systems. Nevertheless, the SL phonons with wave vector parallel to the (001) growth direction, which are those accessible in Raman-backscattering experiments, can, in many cases, be studied with high accuracy within the relatively simple scheme described in detail in this work, and which, yet, can be based on the first-hand information obtained from *ab initio* calculations.

II. LATTICE DYNAMICS OF THE BULK CRYSTALS

A. Phonons in bulk GaAs: One-dimensional representation

Several phenomenological models describing lattice vibrations in bulk GaAs in terms of fitted parameters have been developed in the past: the rigid-ion model,[32] five different versions of shell models,[33,34] and the bond-charge model.[35] Also, as the corresponding computer codes are readily available[36] for most of these models, phonons in bulk GaAs can be generated easily and relatively accurately for an arbitrary wave vector.

In view of the application to (001)-grown superlattices, here we concentrate only on wave vectors $\mathbf{k}=(2\pi/a)(0,0,k_z)$. For wave vectors along this direction, it is then advantageous to think in terms of vibrating (001) atomic planes, each formed by atoms of the same species (Fig. 1), kept together by forces described by interplanar force constants k_n (Fig. 2). We want to point out that a 1D representation in this direction does not imply any approximation, since it can be derived from the conventional 3D description of vibrations through a simple transformation to symmetry coordinates.

The point group leaving $\mathbf{k}=(2\pi/a)(0,0,k_z)$ invariant is C_{2v}, and the decomposition of the representation induced by the basis $u_\alpha(\kappa)$ ($\alpha=x,y,z$ and $\kappa=1$ and 2, respectively for cation and anion) is[37]

$$2\Delta_1+2\Delta_3+2\Delta_4=2A_1+2B_2+2B_1\ , \tag{1}$$

and corresponds to longitudinal (L) and transverse (T_1,T_2) eigenvibrations.

Transformation (A1) in Appendix A block diagonalizes the dynamical matrix, and the eigenvalue problem splits into three 2×2 secular equations, belonging to the symmetries Δ_3, Δ_4, and Δ_1: two transverse and one longitudinal. Every 2×2 block in (A1) can then be thought of as a separate dynamical matrix, belonging to one of the three

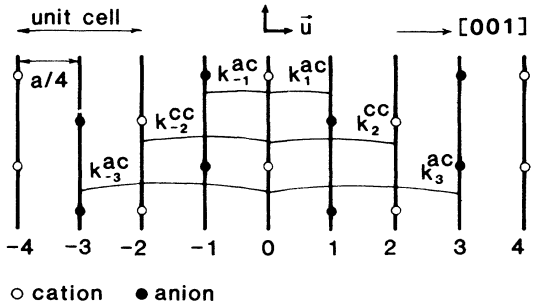

FIG. 2. Some of the interplanar force constants connecting atomic planes perpendicular to the (001) direction. The numbering of the planes is chosen so that the atom at (0,0,0) is in the plane 0, the atom at $(\frac{1}{4},\frac{1}{4},\frac{1}{4})$ in the plane +1, and the plane −1 contains the sites $(\frac{1}{4},-\frac{1}{4},-\frac{1}{4})$ and $(-\frac{1}{4},\frac{1}{4},-\frac{1}{4})$.

symmetries; the corresponding vibrations can be visualized as those of a linear chain of atomic planes, held together by interplanar forces (see Figs. 1 and 2). Interplanar force constants can then be defined as the negative of the force acting on the plane n per unit displacement of the plane 0, i.e.,

$$\mathbf{F}_n = -k_n \mathbf{u}_0 , \tag{2a}$$

and every 2×2 dynamical matrix can be constructed without reference to the original three-dimensional dynamical matrix $\mathbf{C}(\mathbf{k})$ of Eq. (A1), merely as the dynamical matrix of a diatomic linear chain[38] with "springs" $\{k_n\}$ connecting each "atom" to its nth neighbor (Fig. 2).

In the zinc-blende structure the force constants k_n for even n also depend on the atomic species in planes 0 and n (cation-cation or anion-anion); in the following we will either specify additional superscripts (e.g., k_n^{cc}), or use the alternative notation

$$F(l,\kappa) = -\sum_{l',\kappa'} K(l,\kappa;l',\kappa')u(l',\kappa') , \tag{2b}$$

where (l,κ) labels the κth atom in the lth unit cell. The dynamical matrix then may be written as

$$\mathbf{C}^{\rm dyn}(\kappa,\kappa';\mathbf{k}) = (M_\kappa M_{\kappa'})^{-1/2} \sum_{l',\kappa'} K(0,\kappa;l',\kappa')\exp\{(2\pi/a)ik[x(l',\kappa')-x(0,\kappa)]\} , \tag{3}$$

and the eigenmodes are obtained from the secular equation

$$\det\|\mathbf{C}^{\rm dyn}(\mathbf{k}) - [\omega(\mathbf{k})]^2\mathbf{I}_2\| = 0 ; \tag{4}$$

$\mathbf{I}_2$ is the 2×2 identity matrix.

The decomposition of the 3D problem into three 1D problems can be done only within the harmonic approximation, where the force $\mathbf{F}$ and the displacement $\mathbf{u}$ in (2) are parallel; as the displacements have one of the three directions shown in (A2) (transverse or longitudinal), three distinct sets of $\{k_n\}$ are needed to provide a full description of the $\mathbf{k}=(2\pi/a)(0,0,k_z)$ vibrations. In fact, only two of them are significantly different: the longitudinal and transverse sets; the distinction the two transverse types is a matter of labeling only: $k_n(\Delta_4) = k_{-n}(\Delta_3)$. Note that in this description the difference between the $\omega_{\rm LO}(\Gamma)$ and the $\omega_{\rm TO}(\Gamma)$ frequencies results from the difference between the longitudinal and transverse force constants. Moreover, it holds that $k_n \neq k_{-n}$ for T and $k_n = k_{-n}$ for L.[39,40]

Although the $\{k_n\}$ can be related[41] to the usual[42] (interatomic) force constants $\Phi_{\alpha\beta}(l,\kappa;l',\kappa')$ which enter the 3D dynamical matrix $\mathbf{C}(\mathbf{k})$, the relation is of little interest here, as long as we write the 2×2 dynamical matrices directly from $\{k_n\}$, having the 1D picture (Fig. 2) in mind. For GaAs the numerical values of interplanar force constants were determined *ab initio* from definition (2) in Ref. 40, within the Hohenberg-Kohn-Sham local-density approximation; they are given in Table I, and the corresponding dispersion along (001) is shown in Fig. 3 (dashed lines). It is apparent from Table I that the transverse forces extend relatively far, up to the fifth-neighbor plane: this would make any fit to the experimental $\omega(\mathbf{k})$ rather arbitrary.

TABLE I. Interplanar force constants k_n for GaAs as calculated in Ref. 40. In units of 10^5 dyn/cm. The numbering of the planes and the positive sense of the [001] direction are defined in Fig. 2. The transverse force constants given here are pertinent to the Δ_3 symmetry; those for the Δ_4 symmetry can be obtained as $k_n(\Delta_4) = k_{-n}(\Delta_3)$.

Longitudinal (Δ_1)	Transverse (Δ_3)
$k_0^{cc} = 2.038$	$k_0^{cc} = 1.470$
$k_0^{aa} = 1.966$	$k_0^{aa} = 1.760$
$k_{\pm1} = -0.931$	$k_{+1} = -1.470$
	$k_{-1} = -0.127$
$k_{\pm2}^{cc} = -0.117$	$k_{\pm1}^{cc} = 0.095$
$k_{\pm2}^{aa} = -0.081$	$k_{\pm2}^{aa} = -0.020$
$k_{\pm3} = 0.029$	$k_{+3} = -0.019$
	$k_{-3} = -0.076$
$k_{\pm4}^{cc} = 0.000$	$k_{\pm4}^{cc} = 0.028$
$k_{\pm4}^{aa} = 0.000$	$k_{\pm4}^{aa} = -0.002$
$k_{\pm5} = 0.000$	$k_{+5} = -0.018$
	$k_{-5} = -0.006$

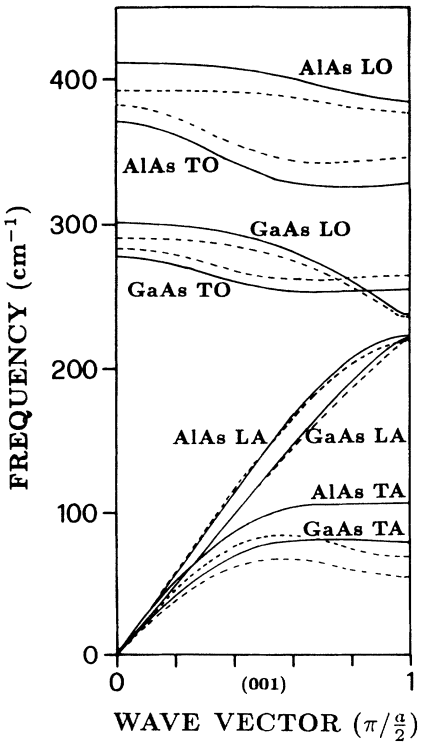

FIG. 3. Bulk dispersion along the [001] direction ($\Gamma \rightarrow X$) for GaAs and AlAs obtained with the force constants of Table I. Dashed lines, "mass approximation"; solid lines, "mass and charge approximation."

On the other hand, the present set of force constants suffers from imprecisions in the *ab initio* determination (due, in particular, to the use of local pseudopotentials and to the limited size of cell used in those early calculations) which are responsible for the somewhat shifted transverse-acoustic (TA) and transverse-optical (TO) branches, as well as for underestimating the splitting between the longitudinal-optical (LO) and the TO modes at point Γ (LO-TO splitting). (See the experimental neutron-scattering data of Refs. 33 and 43.) Besides these problems, which are of essentially computational nature, it is worth noting that the "one-dimensional" description discussed in this subsection is exact, in the sense that no approximation was introduced when going from three dimensions to one dimension. Moreover, we wish to remind the reader that also all "long range" electrostatic interactions are included in the planar forces $\{k_n\}$; the finite LO-TO splitting at point Γ is obtained without using any formal separation into "short-range" and "long-range" interactions, as is customary in the conventional treatment.[44]

B. Phonons in the AlAs: Mass approximation

The details of phonon spectra of AlAs are largely unknown. In the absence of neutron-scattering data, the experimental information is limited to optical measurements,[45] yielding the frequencies only at Γ and X points, and to some recent measurement of sound velocity.[46] The amplitudes of the displacements at point X are available from *ab initio* predictions[47] of frozen phonons using the density-functional formalism. It has been noted,[8,34,48] however, that the known phonons in AlAs can be fairly well described by assuming the same bonding as in GaAs (i.e., the same force constants), with only the cation *masses* modified. As an example, the phonon dispersion in AlAs, calculated in this approximation within one of the shell models for GaAs, is shown in Fig. 4 by dashed lines.

The above finding is not a coincidence: more than a decade ago it was shown[34,48] that for nearly all III-V and II-VI compounds the origin of the most varied shapes of the different phonon dispersions $\omega(\mathbf{k})$ is mainly due to the different *masses* of atoms rather than to different bonding, especially when relating compounds with the same anion (e.g., GaAs↔AlAs, GaSb↔InSb).[48]

In Fig. 3 we show (dashed lines) the AlAs phonons calculated in this "mass approximation" from the GaAs planar force constants of Table I. Obviously, this description combines the imperfections of both approaches: the "mass approximation" and the imperfection of the available set of GaAs planar forces. The main disturbing feature in the $\omega(\mathbf{k})$ of AlAs is the far too narrow LO-TO splitting at Γ.

However imperfect, the mass approximation will introduce a considerable simplification in the description of GaAs/AlAs superlattices: by representing AlAs as merely a mass defect in GaAs, it brings the treatment of the superlattice to that of GaAs with *on-site* perturbations, which do not affect any *interaction* between atoms. This is of special importance in the superlattice, where it considerably simplifies the description of the interactions around the interfaces.

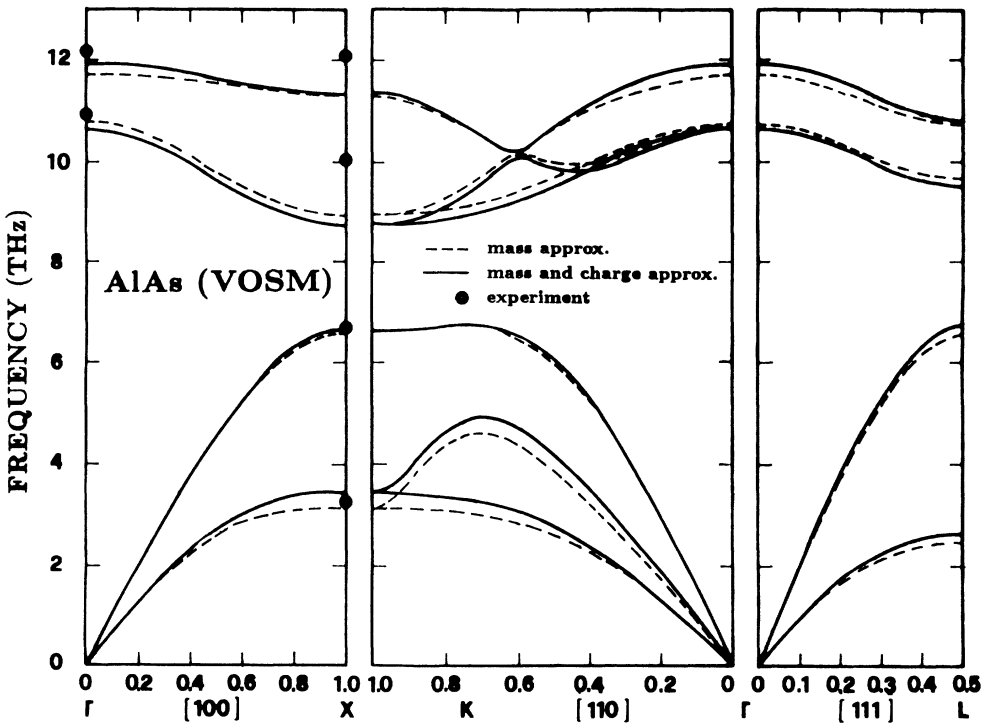

FIG. 4. Bulk dispersions of AlAs calculated with the valence overlap shell model (VOSM) of Ref. 34 assuming the same interactions as in GaAs and the "mass approximation" (dashed lines) or the "mass and charge approximation" (solid lines).

C. Beyond the mass approximation

Although the general shape of the AlAs dispersion is well accounted for by the "mass approximation," the LO-TO splitting at Γ point (Fig. 2) is not reproduced correctly, because it reflects the difference in the microscopic polarizabilities and "deformabilities" of GaAs and AlAs, while the assumption underlying the "mass approximation" is precisely embodied in the equality of Ga and Al potentials. We can improve on this point without abandoning the idea of on-site modifications only.

Let us adopt for a while the framework of phenomenological lattice dynamics; there, the traditional division of forces into "short-range" and Coulomb ones leads to writing the dynamical matrix, in terms of the rigid-ion model (RIM) (Ref. 44) as

$$\mathbf{C}^{\rm dyn}_{\rm GaAs}(\mathbf{k})=\mathbf{C}^{\rm SR}_{\rm GaAs}(\mathbf{k})+\mathbf{M}_1^{-1/2}\mathbf{Z}_1\mathbf{C}^{\rm Coul}(\mathbf{k})\mathbf{Z}_1\mathbf{M}_1^{-1/2}\ , \tag{5}$$

where $\mathbf{C}^{\rm SR}$ is the short-range dynamical matrix and $\mathbf{C}^{\rm Coul}(\mathbf{k})$ is the matrix of Coulomb coefficients (with the macroscopic field included);

$$\mathbf{M}_1=\begin{bmatrix} M({\rm Ga}) & 0 \\ 0 & M({\rm As}) \end{bmatrix}\otimes\mathbf{I}_3 \tag{6}$$

is the matrix of masses;

$$\mathbf{Z}_1=\begin{bmatrix} z^*({\rm Ga}) & 0 \\ 0 & -z^*({\rm Ga}) \end{bmatrix}\otimes\mathbf{I}_3 \tag{7}$$

is the matrix of effective charges, given by

$$(z^*)^2=(\omega_{\rm LO}^2-\omega_{\rm TO}^2)\frac{M_1M_2}{M_1+M_2}\frac{a^3}{16\pi} \tag{8}$$

(Szigeti charge at zero polarizability); and $\cdots\otimes\mathbf{I}_3$ is the direct product with the 3×3 unit matrix. Notice that in our planar-force description z^* only depends on longitudinal and transverse force constants, and the dependence on masses cancels out. Although it is not written explicitly in (5), both $\mathbf{C}^{\rm dyn}$ and $\mathbf{C}^{\rm SR}$ depend on masses $\mathbf{M}_1,\mathbf{M}_2$ as well, in a similar way as the Coulomb part: a matrix multiplied from left and right by $\mathbf{M}_1^{-1/2}$.

The mass approximation discussed in Sec. II B consists of replacing $\mathbf{M}_1$ in (5) by

$$\mathbf{M}_2=\begin{bmatrix} M({\rm Al}) & 0 \\ 0 & M({\rm As}) \end{bmatrix}\otimes\mathbf{I}_3 \tag{9}$$

while keeping all other terms unmodified.

The explicit expression (5) suggests another, somewhat weaker approximation: instead of $\mathbf{C}^{\rm SR}+\mathbf{Z}\mathbf{C}^{\rm Coul}\mathbf{Z}$, we might assume only the $\mathbf{C}^{\rm SR}$ ("short-range" forces) to be equal to both GaAs and AlAs; then, besides the masses, also the matrix of charges would have to be replaced by

$$\mathbf{Z}_2=\begin{bmatrix} z^*({\rm Al}) & 0 \\ 0 & -z^*({\rm Al}) \end{bmatrix}\otimes\mathbf{I}_3\ , \tag{10}$$

with z^*(Al) determined through (8) from the experimental LO,TO (Γ) frequencies of AlAs. Equation (5) then becomes

$$\mathbf{C}^{\rm dyn}_{\rm AlAs}(\mathbf{k})=\mathbf{M}_2^{-1/2}\mathbf{M}_1^{1/2}\mathbf{C}^{\rm SR}_{\rm GaAs}(\mathbf{k})\mathbf{M}_1^{1/2}\mathbf{M}_2^{-1/2}+\mathbf{M}_2^{-1/2}\mathbf{Z}_2\mathbf{C}^{\rm Coul}(\mathbf{k})\mathbf{Z}_2\mathbf{M}_2^{-1/2}\ , \tag{11a}$$

where $\mathbf{C}^{\rm SR}_{\rm GaAs}$ is pertinent to GaAs, $\mathbf{C}^{\rm Coul}(\mathbf{k})$ depends only on the crystal structure, and the $\mathbf{M}_1^{1/2}$ terms "take away" the M(Ga),M(As) dependence from $\mathbf{C}^{\rm SR}_{\rm GaAs}$, in order to let it be replaced by the M(Al),M(As) dependence. Rewriting (11a) as

$$\mathbf{C}^{\rm dyn}_{\rm AlAs}(\mathbf{k})=\mathbf{M}_2^{-1/2}\mathbf{M}_1^{1/2}\mathbf{C}^{\rm dyn}_{\rm GaAs}(\mathbf{k})\mathbf{M}_1^{1/2}\mathbf{M}_2^{-1/2}+\mathbf{M}_2^{-1/2}[\mathbf{Z}_2\mathbf{C}^{\rm Coul}(\mathbf{k})\mathbf{Z}_2-\mathbf{Z}_1\mathbf{C}^{\rm Coul}(\mathbf{k})\mathbf{Z}_1]\times\mathbf{M}_2^{-1/2}\ , \tag{11b}$$

the artificial division of forces into "short range" and "long range" is no longer needed: we can identify $\mathbf{C}^{\rm dyn}_{\rm GaAs}(\mathbf{k})$ in (11b) with the dynamical matrix constructed within some scheme more sophisticated than the RIM, such as a shell model or the *ab initio* scheme of Ref. 40, so that only the *difference* between the interactions in GaAs and AlAs is treated within the RIM. Whenever $\mathbf{Z}_2\neq\mathbf{Z}_1$, we refer to (11b) as "mass and charge approximation."

As an example, the dispersion of AlAs—calculated with the (valence-overlap) shell model (VOSM) of Kunc and Bilz[34] for $\mathbf{C}^{\rm dyn}_{\rm GaAs}(\mathbf{k})$—is shown in Fig. 4 by solid lines.

In order to use the "mass and charge approximation" within the "one-dimensional" description in terms of the interplanar forces, we have to apply the transformations (A1) and (A2), which block diagonalize the 3D dynamical matrix, also to the Coulomb matrix $\mathbf{C}^{\rm Coul}$. While the explicit block diagonalization of $\mathbf{C}^{\rm dyn}$ is not needed (one directly writes the "small" dynamical matrices for the linear chain, using interplanar force constants), the result of block diagonalization of the Coulomb part $\mathbf{C}^{\rm Coul}(\mathbf{k})$ will be discussed in Sec. III.

Anticipating the results, the phonon dispersion in AlAs calculated by this method with planar force constants of GaAs (Ref. 40) is shown in Fig. 3 by solid lines. (Here the effective charge of AlAs was taken to be $0.763|e|$, as deduced from the LO-TO splitting in Ref. 45.)

Now the charge approximation not only yields the correct LO-TO splitting, but it also straightens the TA dispersion. Notice, however, the shift of the LO and TO branches; its amount is not large and its experimental value depends on the temperature.

A similar treatment can also be applied to GaAs, for the force constants of Table I give a too small LO-TO splitting at point Γ: its value corresponds to the effective charge of $0.367|e|$, as compared with the actual experimental value of $0.673|e|$, calculated through Eq. (8) from measurements of Ref. 33.

Writing (11b) with $\mathbf{M}_1=\mathbf{M}_2$, and evaluating the right-hand side with $0.367|e|$ and $0.673|e|$ for Z_1 and Z_2, respectively, and with force constants from Table I, we obtain the GaAs phonon dispersion depicted in Fig. 3 by solid lines, which shows the same kind of changes as in AlAs (shown in Fig. 3). However, here also the modification of the effective charges produces some change in the dispersion (shift plus broadening of band

width). The modification of the eigenvectors is, on the other hand, negligible.

In our approach Table I is thus seen merely as a "reference set" of force constants (rather than an actual representation of GaAs) and the "mass and charge approximation" (11b) is written in a somewhat more general form:

$$\mathbf{C}_{\rm act}^{\rm dyn}(\mathbf{k}) = \mathbf{M}_{\rm act}^{-1/2}\mathbf{M}_{\rm ref}^{1/2}\mathbf{C}_{\rm ref}^{\rm dyn}(\mathbf{k})\mathbf{M}_{\rm ref}^{1/2}\mathbf{M}_{\rm act}^{-1/2} + \mathbf{M}_{\rm act}^{-1/2}[\mathbf{Z}_{\rm act}\mathbf{C}^{\rm Coul}(\mathbf{k})\mathbf{Z}_{\rm act} - \mathbf{Z}_{\rm ref}\mathbf{C}^{\rm Coul}(\mathbf{k})\mathbf{Z}_{\rm ref}]\mathbf{M}_{\rm act}^{-1/2} , \quad (12)$$

where the subscript "act" stands for the actual compound in question (GaAs or AlAs), and "ref" denotes the reference system (presently GaAs as characterized by the force constants of Table I).

Notice that, in practice, dealing with the "mass and charge approximation" of Eq. (12) is not more involved than dealing with the "mass approximation," once the Coulomb matrix is known; also, the "mass and charge approximation" retains the most prominent feature of the "mass approximation," i.e., the "perturbation" ($\mathbf{Z}_{\rm ref}\rightarrow\mathbf{Z}_{\rm act}$) is still localized *on the sites* and does not affect pair interactions. It will be shown in the next section that the Coulomb matrix can be generated in a simple way, formally analogous to the construction of the dynamical matrix from interplanar force constants.

We note that the applicability of the approximation in Eq. (12) is not restricted to the GaAs↔AlAs relation only; the relation GaSb↔InAs has already been tested in Ref. 17 following the treatment outlined in the present paper. It would be worth checking how many different phonon dispersions can be generated from a single set of force constants, and how precisely, by simply varying masses and controlling the LO-TO splitting.

III. DYNAMICAL MATRIX FOR GaAs/AlAs SUPERLATTICES IN THE MASS AND CHARGE APPROXIMATION

The one-dimensional representation in terms of planar constants lends itself to an easy extension to a GaAs/AlAs superlattice: as shown in the previous sections, the interactions can be assumed to be identical all along the superlattice, and only masses and charges are modified from one component to the other. While the extension of Sec. II B to the case of superlattices is straightforward in the mass approximation, the treatment of the corrective Coulomb term used in the charge approximation merits some caution. It is useful to return for a moment to the standard three-dimensional formulation.

For a general 3D lattice, the dynamical matrix within the RIM may be written as

$$C_{\alpha\beta}^{\rm dyn}(\kappa,\kappa';\mathbf{k}) = C_{\alpha\beta}^{\rm SR}(\kappa,\kappa';\mathbf{k}) + \frac{4\pi}{v_c}\frac{k_\alpha k_\beta}{|\mathbf{k}|^2}\frac{Z_\kappa Z_{\kappa'}}{(M_\kappa M_{\kappa'})^{1/2}} - \frac{Z_\kappa Z_{\kappa'}}{(M_\kappa M_{\kappa'})^{1/2}}Q_{\alpha\beta}(\kappa,\kappa';\mathbf{k}) + \delta_{\kappa\kappa'}\frac{Z_\kappa}{M_\kappa}\sum_{\kappa''}Z_{\kappa''}Q_{\alpha\beta}(\kappa,\kappa'';\mathbf{k}=\mathbf{0}) \quad (13)$$

[see Eq. (31.17) of Ref. 44], where v_c is the volume of the unit cell. Here the second term corresponds to the macroscopic electric field, and $Q(\mathbf{k})$ are the "nondivergent" Coulomb coefficients.

The second and third terms are the elements of $\mathbf{C}^{\rm Coul}(\mathbf{k})$ which already appeared in Eq. (5), i.e.,

$$C_{\alpha\beta}^{\rm Coul}(\kappa,\kappa';\mathbf{k}) = \frac{4\pi}{v_a}\frac{k_\alpha k_\beta}{|\mathbf{k}|^2} - Q_{\alpha\beta}(\kappa,\kappa';\mathbf{k}) . \quad (14)$$

The last term in (13) guarantees the translational invariance of the dynamical matrix; it is zero by symmetry in the bulk zinc-blende structure, but not in a superstructure, when there are two different sets of effective charges.

With this in mind, the dynamical matrix for the $(\mathrm{GaAs})_m/(\mathrm{AlAs})_n$ superlattice in the "mass and charge approximation" reads like the dynamical matrix of the bulk—Eq. (12)—but with the $Q(\mathbf{k}=\mathbf{0})$ term added:

$$\mathbf{M}_{\rm act}^{1/2}\mathbf{C}_{\rm act}^{\rm dyn}(\mathbf{k})\mathbf{M}_{\rm act}^{1/2} = \mathbf{M}_{\rm ref}^{1/2}\mathbf{C}_{\rm ref}^{\rm dyn}(\mathbf{k})\mathbf{M}_{\rm ref}^{1/2} + [\mathbf{Z}_{\rm act}\mathbf{C}^{\rm Coul}(\mathbf{k})\mathbf{Z}_{\rm act} - \mathbf{Z}_{\rm ref}\mathbf{C}^{\rm Coul}(\mathbf{k})\mathbf{Z}_{\rm ref}] + f(\mathbf{k}=\mathbf{0}) , \quad (15a)$$

where

$$f_{\alpha\beta}(\kappa,\kappa';\mathbf{k}=\mathbf{0}) \equiv \delta_{\kappa\kappa'}Z_\kappa\sum_{\kappa''}Z_{\kappa''}Q_{\alpha\beta}(\kappa,\kappa'';\mathbf{k}=\mathbf{0}) , \quad (15b)$$

and wherever the superscript "ref" or "act" is missing, it is understood that $Z \equiv Z_{\rm act}$. A term like (15b) with $\mathbf{Z}\equiv\mathbf{Z}_{\rm ref}$ is not written in (15a) because the reference system is zinc-blende $(\mathrm{GaAs})_{m+n}$ and symmetry makes it vanish. The Coulomb matrices $\mathbf{C}^{\rm Coul}$ will be discussed later.

A simple way of evaluating expression (15b) is to calculate the dynamical matrix as in Eq. (12) at $\mathbf{k}=\mathbf{0}$ and to "correct" the diagonal elements so as to make the elements of each line sum to zero (condition of translational invariance). The correction term found in this way at $\mathbf{k}=\mathbf{0}$ can then be used in the dynamical matrix at any $\mathbf{k}$.

The diagonal matrices $\mathbf{M}$ and $\mathbf{Z}$ contain the actual masses and effective charges, as they occur along the superlattice. The variation of the effective charge along the superlattice is to some extent a matter of assumption: deep in the interior of each layer, one can expect the effective charges to be the same as in bulk GaAs or AlAs. When approaching the interface, however, one expects the $\pm Z_{\rm GaAs}$ to go, smoothly or abruptly, into $\pm Z_{\rm AlAs}$. As no individual atomic values are accessible to direct measurement, we adopt the hypothesis that the interface As atom, which is "common" to both components, carries an effective charge which is the average of those in GaAs and AlAs bulks; for all other atoms the "regular" bulk values of z^* are taken. A few test calculations have shown that reasonable changes in this assumption around

TABLE II. $e^2\times$(Coulomb coefficients) (see Appendix B) calculated by Ewald summation for $(0,0,k_z)\rightarrow(0,0,0)$ and lattice constant $a=5.65$ Å. In units of 10^5 dyn/cm. The conventions for the numbering of the planes are as in Table I. In order to obtain the planar force constants corresponding to Coulomb interactions in Eqs. (12) and (15a), one multiplies the a_i,b_i from the table by the charges Z in atu. (When expressed in units of e^2/v_c, these planar Coulomb interactions are universal coefficients for the zinc-blende structure, independent of the lattice constant a.)

Longitudinal (Δ_1)	Transverse (Δ_3)
$a_0=0.326\,80$	$b_0=-0.163\,40$
$a_{\pm1}=0.213\,67$	$b_{+1}=-0.374\,83$
	$b_{-1}=0.161\,16$
$a_{\pm2}=0.051\,71$	$b_{\pm2}=-0.025\,86$
$a_{\pm3}=0.000\,63$	$b_{+3}=0.003\,32$
	$b_{-3}=-0.003\,96$
$a_{\pm4}=-0.000\,82$	$b_{\pm4}=0.000\,41$
$a_{\pm5}=0.000\,00$	$b_{+5}=-0.000\,04$
	$b_{-5}=0.000\,04$

the interface have a negligible effect on the eigenfrequencies.

The Coulomb coefficients depend only on the crystal structure [zinc-blende, $(m+n)$-times supercell] and not on the atomic species occupying the sites. The $6(m+n)\times6(m+n)$ matrices $\mathbf{C}^{\mathrm{Coul}}$ are easily evaluated by Ewald summation[49] in three dimensions; they are then transformed by the matrices **P** and **U** [Eqs. (A1)–(A3)] with $\mathbf{I}_2$ replaced by $\mathbf{I}_{2(m+n)}$ to the form compatible with the linear-chain equation (5), and can be viewed as "Coulomb coefficients in one dimension." The resulting Coulomb matrix shows a regular pattern, in analogy with the dynamical matrix (see Appendix B). In particular, it shows a structure in bands, such that all the atoms which are nth neighbors are coupled by the same coefficient. The important finding is that these coefficients decrease with the distance between the planes, and that they are *short ranged*: they extend essentially to the third- to fifth-neighbor planes.[12] The Coulomb coefficients of Ref. 12 are reported here for convenience in Table II. Their short range demonstrates one advantage of dealing with planes of atoms rather than with individual atoms, and is a consequence of the fact that dipole-dipole interactions between planes decay faster than those between individual atoms (see Ref. 50).

This allows us to deal with the Coulomb coefficients as with interplanar Coulomb force constants originating from purely electrostatic interaction. This fact brings about a dramatic simplification: the phonons of a superlattice of *any* thickness at *any* **k** can be calculated in terms of the force constants of Table I and of the small number of Coulomb coefficients given in Table II, and by imposing translational invariance.

IV. CALCULATED SUPERLATTICE PHONON SPECTRA

We have discussed elsewhere several aspects of the phonon spectra of GaAs/AlAs, obtained with the present approach. In particular, the frequencies of confined optical modes and their relation with the bulk dispersion have been described in Refs. 11, 12, and 1(c). Selected displacement patterns for both longitudinal and transverse polarizations are also shown in Refs. 11 and 13. A critical discussion of the comparison between theory and experiments, and of the possible role of interfaces for (001)-propagating modes is given in Ref. 1(c). This reference also presents a comparison between GaAs/AlAs SL's and SL's made of other materials. The easy applicability of the present method to systems with a very large number of atomic planes was demonstrated in Ref. 15 by studying finite SL's with ideal unreconstructed surfaces. In that case, it was shown how the availability of displacements allows one to perform a model calculation of Raman intensities easily.

We give here a few more applications with the purpose of illustrating the method. In order to clarify the transition from bulk to superlattice, we show in Fig. 5 the thinnest possible superlattice, a $(GaAs)_1/(AlAs)_1$ periodic sequence; although this is an extreme configuration, its modes can still be to some extent related to the bulk modes of the two materials. The folding due to the doubled periodicity brings the branches labeled with primes into the new Brillouin zone (BZ) (extending from point Γ to $x/2$), the modes of the previous zone boundary at point X now being at point Γ. However, the substitution Ga→Al results in the splitting of the folded modes at the new BZ boundary and in shifts of the "folded" branches. While the small splitting of the acoustic branches can still be considered a perturbation, the effect on optical modes is so strong that the idea of folding—implying small deviation from continuity of the branches at the zone boundary—becomes meaningless. This is even more evi-

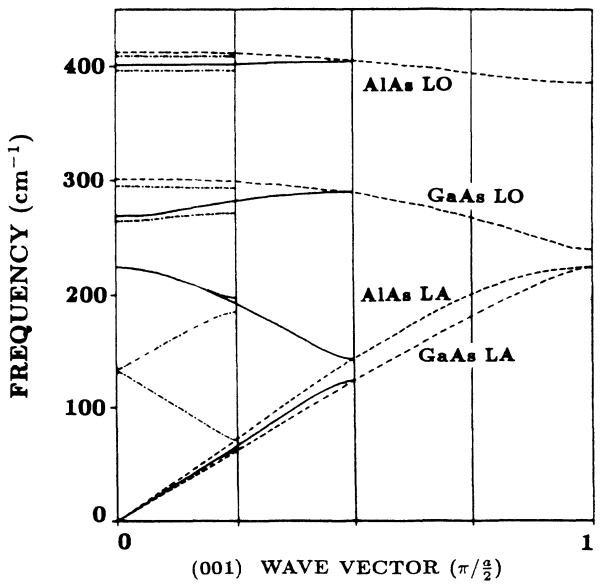

FIG. 5. Longitudinal dispersion of the $(GaAs)_1/(AlAs)_1$ (solid lines) and $(GaAs)_2/(AlAs)_2$ (dashed-dotted lines) superlattices grown along [001]. The [001] dispersions of the bulk GaAs and AlAs constituents are also shown (dashed lines) to illustrate the origin of the different superlattice branches.

dent for $(GaAs)_2/(AlAs)_2$, also displayed in Fig. 5. Here, contrary to acoustic modes, the optical ones have become almost dispersionless, so that the relation with the original bulk modes is not longer easy to trace back. This essential difference between folded acoustic and "folded" optical modes is visible on the displacement patterns in Fig. 6; the folded acoustic modes keep their acoustic character, cations and anions moving in phase. The almost overlapping ranges of bulk GaAs and AlAs LA frequencies make the folded acoustic modes propagate through the whole superlattice. This contrasts with the behavior of the optical modes (Fig. 6), which are essentially confined in one layer or the other; since their eigenfrequencies fall outside the bands of allowed frequencies of either GaAs or AlAs, their amplitudes are strongly reduced in the GaAs and AlAs layers, respectively. This is why they are usually referred to as GaAs-like or AlAs-like confined modes.

It is interesting to note that for the same reasons confined AlAs-like modes can appear also in the acoustic range of frequency, since the AlAs transverse-acoustic continuum extends to higher frequency than that of GaAs. In other words, the interval between the TA(X) of GaAs and the TA(X) of AlAs is forbidden for vibrations of GaAs, and only allowed for AlAs-like modes.

The two cases described up to now are peculiar since the layers are thinner than the range of interactions, so that successive layers of the same material still interact directly with each other. Next, we present results for the L polarization in a $(GaAs)_4/(AlAs)_4$ superlattice, where this is no longer the case. In Fig. 7 we show the frequency spectrum of the superlattice and the corresponding displacement patterns at the Γ point. Indeed, the character of confined and extended modes becomes very apparent here.

Let us focus on optical modes: the confinement is more pronounced for the AlAs-like than for the GaAs-like ones, and for transverse modes more than for longitudinal ones. Moreover, the confinement of the LO GaAs-like modes increases with increasing frequency.

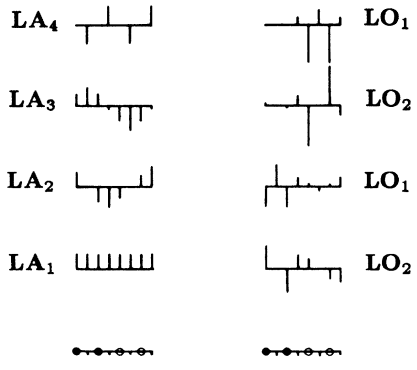

FIG. 6. Amplitude of the longitudinal Γ-point displacements for the four acoustic modes (LA, left panel) and the four optical (LO, right panel) modes of a $(GaAs)_2/(AlAs)_2$ superlattice. In the right panel, the two topmost modes are AlAs-like and the two lowest are GaAs-like. (The geometry of the atomic planes is shown at the bottom: tics represent As atomic planes, solid circles Ga planes, and open circles Al planes.)

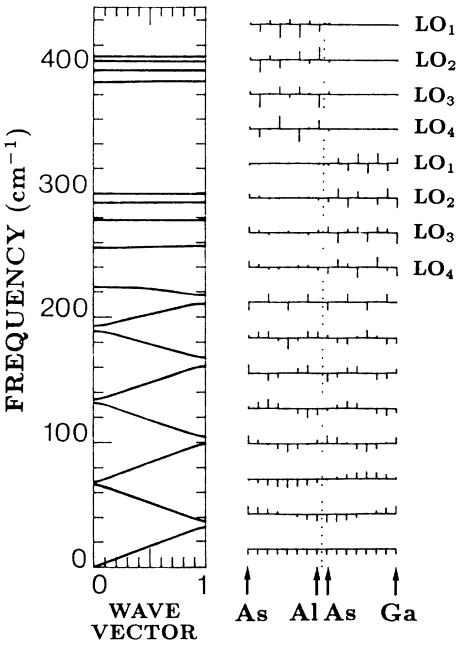

FIG. 7. Longitudinal dispersion of the $(GaAs)_4/(AlAs)_4$ (001) superlattice (left), with the corresponding amplitude of Γ-point displacements (right). From top to bottom, in order of decreasing frequency, are the four LO AlAs-like modes, the four LO GaAs-like modes, and the acoustic modes.

All this can be understood in terms of complex branch dispersion of the bulk constituents.[9] For instance, the lowest GaAs-like optical mode would be strictly confined in the TO case, where the allowed bulk continua of AlAs are very far away, whereas in the LO case the corresponding mode spills substantially into AlAs since the

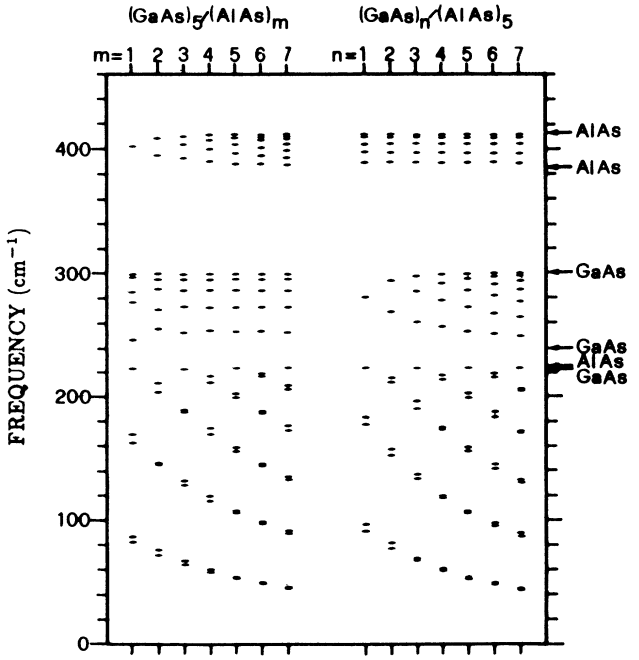

FIG. 8. Dependence of the Γ-point frequencies of GaAs/AlAs superlattices vs the thickness of one layer when the other is kept at the constant thickness of 5 monolayers. The arrows on the right-hand side represent the edges of the bulk-phonon continua.

AlAs acoustic continuum lies very close in energy.

The transverse case is very similar.[11] The only new feature is the appearance of several confined acoustic modes in the range between the bulk TA(X) frequency of GaAs and AlAs. It would be interesting to test the existence of these confined acoustic modes experimentally, by checking the Raman enhancement under resonance conditions with one material or another.

Finally, in Fig. 8 we show the dependence of the Γ-point frequency of all modes on the thickness of one layer when the thickness of the other is kept fixed. The characteristic behavior of optical modes confirms their confined character: the AlAs (GaAs) -like modes remain constant when the adjacent GaAs (AlAs) thickness is varied, while their frequency decreases when the thickness of the AlAs (GaAs) layer itself is decreased.

The stronger confinement of AlAs-like LO modes compared to the GaAs-like ones is confirmed by the fact that they are not influenced by the decrease in the thickness of the GaAs barrier, not even when it reaches its thinnest extreme; the GaAs-like modes, instead, are appreciably sensitive to a decrease in the thickness of the AlAs barrier below 4 monolayers.

In summary, we have given a detailed description of a method which allows one to calculate the phonon spectra of (001)-grown superlattices along the growth direction. We have shown how a one-dimensional (linear-chain) representation can include also long-range forces and how it can be used for a simple and quantitative description of superlattice phonon spectra.

Note added in proof. A recent paper[51] provides new dispersions of bulk GaAs and AlAs, calculated *ab initio* within linear response theory, using norm-conserving pseudopotentials. These dispersions are probably more accurate than the ones we are using (taken from the very first *ab initio* calculations, Ref. 40), and show some significant difference particularly for what concerns the flat AlAs LO branch. However, a "mass and charge approximation" relation between GaAs and AlAs holds also for these new results (already with $Z_{\rm act}=Z_{\rm ref}$, i.e., with the simple "mass approximation," the AlAs dispersion can be obtained with good accuracy from the GaAs force constants[51]), and therefore we believe that the validity and practical use of our approach is—if ever—increased by the possibility of combining it with new improved sets of force constants.

ACKNOWLEDGMENTS

This work was supported in part by the Consiglio Nazionale delle Ricerche (CNR) through the national project for vectorial computation in physics (Italy) and by the Centre de Calcul Vectoriel pour la Recherche (CCVR) (Palaiseau, France). The SNCI (Service National de Champs Intenses) is Laboratoire associé à l'Université Joseph Fourier de Grenoble, France.

APPENDIX A

All representations in Eq. (1) are one dimensional, and the last two are degenerate by time-reversal invariance; the 6×6 dynamical matrix $\mathbf{C}(\mathbf{k})$ can be brought into symmetry coordinates by the transformation

$$\mathbf{P}^{-1}\mathbf{U}^{-1}\mathbf{C}^{\rm dyn}(\mathbf{k})\mathbf{U}\mathbf{P}\ . \tag{A1}$$

The matrix

$$\mathbf{U}=\mathbf{I}_2\otimes\begin{bmatrix}1/\sqrt{2} & 1/\sqrt{2} & 0\\ 1/\sqrt{2} & -1/\sqrt{2} & 0\\ 0 & 0 & 1\end{bmatrix} \tag{A2}$$

has the symmetry coordinates $(\Delta_3,\Delta_4,\Delta_1)$ for its columns, and the u_x,u_y,u_z components as rows; $\mathbf{I}_2\otimes\cdots$ stands for the direct product with the 2×2 identity matrix. The multiplications by the permutation matrix,

$$\mathbf{P}=\begin{bmatrix}1&0&0&0&0&0\\0&0&1&0&0&0\\0&0&0&0&1&0\\0&1&0&0&0&0\\0&0&0&1&0&0\\0&0&0&0&0&1\end{bmatrix}, \tag{A3}$$

merely mean interchanging rows and columns in order to bring together the elements belonging to the same representations (viz., in the order $\Delta_3,\Delta_4,\Delta_1$).

APPENDIX B

The $6m\times6m$ Coulomb matrix $\mathbf{C}^{\rm Coul}(\mathbf{k})$—Eq. (14)—for the zinc-blende structure described by the (001) supercell $(\mathrm{GaAs})_m$ can be brought into symmetry coordinates by the transformation (A1) (with $\mathbf{I}_2$ replaced by $\mathbf{I}_{2m}$), and it decomposes into three matrices: (i) a cyclic matrix,

$$\begin{bmatrix}a_0 & a_1 & a_2 & \cdots & a_2^* & a_1^*\\ & a_0 & a_1 & \cdots & & a_2^*\\ & & a_0 & & & \\ & & & \ddots & \vdots & \vdots\end{bmatrix}, \tag{B1}$$

which corresponds to the longitudinal modes (Δ_1), and (ii) a band matrix,

$$\begin{bmatrix}b_0 & b_{+1} & b_2 & & \cdots & b_2^* & b_{-1}^*\\ & b_0 & b_{-1} & b_2 & \cdots & & b_2^*\\ & & b_0 & b_{+1} & & & \\ & & & & \ddots & \vdots & \vdots\end{bmatrix}, \tag{B2}$$

corresponding to the transverse Δ_3 modes. The third matrix, pertinent to the Δ_4 symmetry, can be obtained from (B2) by interchanging the elements $b_n\leftrightarrow b_{-n}$ in the bands with odd n.

In the $(0,0,k_z)\rightarrow(0,0,0)$ limit, all the coefficients become real numbers and can be viewed as longitudinal or transverse *force constants* relating to Fig. 2 and satisfying the relations: $a_{+n}=a_{-n}$ (longitudinal) and $b_{2n}^{aa}=b_{2n}^{cc}$ (transverse). (Unlike the actual force constants k_n, the Coulomb planar forces must be the same for cation-cation and anion-anion interactions). The numerical values of a_n and b_n, calculated for $k_z\rightarrow0$ along the [001] direction by the usual Ewald summation in three dimensions[42,44,49] on the (001) supercell $(\mathrm{GaAs})_{14}$ with $a=5.65$

Å for lattice constant, are given in Table II. They decrease rapidly with the interplanar distance, so that the nonzero bands "on the left" and "on the right" in (B1) and (B2) are separated by several (17–19) bands of zeros.

Viewing the a_n and b_n of Table II as planar force constants allows one to calculate the Coulomb matrix $\mathbf{C}^{\mathrm{Coul}}(\mathbf{k})$ for *any* n, as a *dynamical matrix*, i.e., through formula (3), rather than by a new Ewald summation. This interpretation also allows one to construct the matrices (B1) and (B2) easily, even when $m \leq 5$, i.e., when the bands "on the left" and "on the right" are no longer separated by zeros but they overlap.

---

*Present and permanent address: Scuola Internazionale Superiore di Studi Avanzati (SISSA), strada Costiera 11, I-34114 Trieste, Italy.

[1]For recent reviews, see (a) M. V. Klein, IEEE J. Quantum Electron. **QE-22**, 1760 (1986); (b) B. Jusserand and M. Cardona, in *Light Scattering in Solid V*, edited by M. Cardona and G. Güntherodt (Springer, Berlin, 1989), p. 49; (c) A. Fasolino and E. Molinari, in Proceedings of the IVth International Conference on Modulated Semiconductor Structures (MSS-IV), Ann Arbor, 1989 [Surf. Sci. (to be published)].

[2]G. Fasol, M. Tanaka, H. Sakaki, and Y. Horikoshi, Phys. Rev. B **38**, 6056 (1988).

[3]D. Levi, Shu-Lin Zhang, M. V. Klein, J. Klem, and H. Morkoç, Phys. Rev. B **36**, 8032 (1987).

[4]See, e.g., Z. P. Wang, D. S. Jiang, and K. Ploog, Solid State Commun. **65**, 661 (1988); T. A. Gant, M. Delaney, M. V. Klein, R. Houdré, H. Morkoç, Phys. Rev. B **39**, 1696 (1989), and references therein.

[5]See, e.g., R. Merlin, in *Light Scattering in Solids V*, edited by M. Cardona and G. Güntherodt (Springer, Berlin, 1989).

[6]See, e.g., K. Eberl, G. Grötz, R. Zachai, and G. Abstreiter, J. Phys. (Paris) Colloq. **48**, C5-329 (1987); J. C. Tsang, S. S. Iyer, and S. L. Delage, Appl. Phys. Lett. **51**, 1732 (1987); D. J. Lockwood, M. W. C. Dharma-wardana, G. C. Aers, and J. M. Baribeau, Appl. Phys. Lett. **52**, 2040 (1988); M. Ospelt, W. Bacsa, J. Henz, K. A. Mäder, and H. Von Känel, in Proceedings of the IVth International Conference on Superlattices, Microstructures and Microdevices, Trieste, 1988 [Superlatt. Microstruct. **5**, 71 (1989)]; J. Menéndez, A. Pinczuk, J. Bevk, and J. P. Mannaerts, J. Vac. Sci. Technol. B **6**, 1306 (1988).

[7]See, e.g., J. M. Gérard, J. Y. Marzin, B. Jusserand, F. Glas, and J. Primot, Appl. Phys. Lett. **54**, 30 (1989).

[8]A. S. Barker, Jr., J. L. Merz, and A. C. Gossard, Phys. Rev. B **17**, 3181 (1978).

[9]C. Colvard, T. A. Gant, M. V. Klein, R. Merlin, R. Fischer, H. Morkoç, and A. C. Gossard, Phys. Rev. B **31**, 2080 (1985).

[10]B. Jusserand, D. Paquet, and A. Regreny, Phys. Rev. B **30**, 6245 (1984).

[11]E. Molinari, A. Fasolino, and K. Kunc, in *Proceedings of the 18th International Conference on the Physics of Semiconductors, Stockholm, 1986*, edited by O. Engström (World Scientific, Singapore, 1987), p. 663.

[12]E. Molinari, A. Fasolino, and K. Kunc, Superlatt. Microstruct. **2**, 397 (1986).

[13]E. Molinari, A. Fasolino, and K. Kunc, Phys. Rev. Lett. **56**, 1751 (1986).

[14]E. Molinari and A. Fasolino, Superlatt. Microstruct. **4**, 449 (1988).

[15]L. Sorba, A. Molinari, and A. Fasolino, Surf. Sci. **211/212**, 354 (1989).

[16]A. Fasolino, E. Molinari, and J. C. Maan, Phys. Rev. B **33**, 8889 (1986).

[17]A. Fasolino, E. Molinari, and J. C. Maan, Superlatt. Microstruct. **3**, 117 (1987).

[18]E. Molinari, A. Fasolino, and J. C. Maan, Phys. Rev. B **39**, 3923 (1989).

[19]A. Fasolino and E. Molinari, J. Phys. (Paris) Colloq. **48**, C5-569 (1987).

[20]E. Molinari and A. Fasolino, Appl. Phys. Lett. **54**, 1220 (1989).

[21]S. F. Ren, H. Chu, and Y. C. Chang, Phys. Rev. B **37**, 8899 (1988).

[22]E. Richter and D. Strauch, Solid State Commun. **64**, 867 (1987).

[23]T. Tsuchiya, H. Akera, and T. Ando, Phys. Rev. B **39**, 6025 (1989).

[24]G. Kanellis, Phys. Rev. B **35**, 746 (1987).

[25]F. Bechstedt and H. Gerecke, Phys. Status Solidi B **156**, 151 (1989).

[26]L. Colombo and L. Miglio, Surf. Sci. (to be published).

[27]R. Merlin, C. Colvard, M. V. Klein, H. Morkoç, A. Y. Cho, and A. C. Gossard, Appl. Phys. Lett. **36**, 43 (1980).

[28]A. K. Sood, J. Menéndez, M. Cardona, and K. Ploog, Phys. Rev. Lett. **54**, 2111 (1985); **54**, 2115 (1985).

[29]R. E. Camley and D. L. Mills, Phys. Rev. B **29**, 1695 (1984).

[30]R. Enderlein and F. Bechstedt, in *Proceedings of the 18th International Conference on the Physics of Semiconductors, Stockholm, 1986*, Ref. 11, p. 655.

[31]S. Baroni, P. Giannozzi, and E. Molinari, in *Proceedings of the 19th International Conference on the Physics of Semiconductors, Warsaw, 1988*, edited by W. Zawadzki (Institute of Physics/Polish Academy of Sciences, Warsaw, 1988), p. 795; in *Proceedings of the Third International Conference on Phonon Physics, Heidelberg, 1989* (World Scientific, Singapore, in press).

[32]K. Kunc, M. Balkanski, and M. A. Nusimovici, Phys. Rev. B **12**, 4346 (1975); Phys. Status Solidi B **72**, 229 (1975).

[33]G. Dolling and J. L. T. Waugh, in *Lattice Dynamics*, edited by R. F. Wallis (Pergamon, London, 1965), p. 19.

[34]K. Kunc and H. Bilz, Solid State Commun. **19**, 1927 (1976); K. Kunc and H. Bilz, in *Proceedings of the International Conference on Neutron Scattering, Gatlinburg, 1976*, edited by R. M. Moon (Oak Ridge National Laboratory, Oak Ridge, 1976), p. 195.

[35]K. C. Rustagi and W. Weber, Solid State Commun. **18**, 673 (1976).

[36]K. Kunc and O. H. Nielsen, Comput. Phys. Commun. **17**, 413 (1979).

[37]For the notation see: G. F. Koster, in *Solid State Physics*, edited by H. Ehrenreich, F. Seitz, and D. Turnbull (Academic, New York, 1957), Vol. 5, p. 173.

[38]C. Kittel, *Introduction to Solid State Physics*, 5th ed. (Wiley, New York, 1976), p. 112.

[39]The microscopic origin of this different behavior is that longitudinal displacement of an atomic plane bends and compresses the interatomic bonds on its left as much as it unbends and stretches the ones on its right, which in the harmonic approximation produces the same effect; a transverse

displacement, on the other hand, mostly stretches the bonds on one side and mostly bends those on the other side, giving rise to very different force constants. See Ref. 40.

[40]K. Kunc and R. M. Martin, Phys. Rev. Lett. **48**, 406 (1982); K. Kunc, in *Electronic Structure, Dynamics and Quantum Structural Properties of Condensed Matter,* edited by J. T. Devreese and P. E. Van Camp (Plenum, New York, 1985), p. 221.

[41]A. Fleszar and R. Resta, Phys. Rev. B **34**, 7140 (1986); L. Colombo and L. Miglio (unpublished).

[42]A. Maradudin, E. W. Montroll, G. H. Weiss, and I. P. Ipatova, *Theory of Lattice Dynamics in the Harmonic Approximation,* Suppl. 3 of *Solid State Physics,* edited by H. Ehrenreich, F. Seitz, and D. Turnbull (Academic, New York, 1971).

[43]D. Strauch and B. Dorner, J. Phys. Condens. Matter **2**, 1457 (1990).

[44]M. Born and K. Huang, *Dynamical Theory of Crystal Lattice* (Clarendon, Oxford, 1954).

[45]A. Onton, in *Proceedings of the 10th International Conference Physics of Semiconductors,* edited by S. P. Keller, J. C. Hensel, and F. K. Stern (U.S. AEC, New York, 1970), p. 107; B. Monemar, Phys. Rev. B **8**, 5711 (1973).

[46]H. T. Grahan, D. A. Young, H. J. Maris, J. Tauc, J. M. Hong, and T. P. Smith, Appl. Phys. Lett. **53**, 2023 (1988).

[47]K. J. Chang and M. L. Cohen, in *Proceedings of the 17th International Conference Physics on the Physics of Semiconductors,* edited by J. D. Chadi and W. A. Harrison (Springer-Verlag, New York, 1985), p. 1151.

[48]N. Meskini and K. Kunc, Université Pierre et Marie Curie, Technical Report No. 5, 1978 (unpublished).

[49]P. P. Ewald, Ann. Phys. (Leipzig) [Folge 4] **54**, 519 (1917); [Folge 4] **64**, 253 (1921).

[50]J. E. Lennard-Jones and B. M. Dent, Trans. Faraday Soc. **24**, 92 (1928).

[51]S. Baroni, P. Giannozzi, and E. Molinari, Phys. Rev. B **41**, 3870 (1990); see also P. Pavone, Master thesis, SISSA, Trieste, 1990.